Pergamon

Int. J. Heat Mass Transfer. Vol. 40, No. 16, pp. 3849–3860, 1997

Printed in Great Britain
0017–9310/97 $17.00+0.00

PII: S0017–9310(97)00043–4

Turbulent natural convection heat transfer in an asymmetrically heated, vertical parallel-plate channel

A. G. FEDOROV and R. VISKANTA†

Heat Transfer Laboratory, School of Mechanical Engineering, Purdue University, West Lafayette, IN 47907, U.S.A.

(*Received* 25 *September* 1996 *and in final form* 14 *January* 1997)

Abstract—An analysis has been developed to predict induced flow and heat transfer in an asymmetrically heated, vertical parallel-plate channel. The problem considered is related to numerous industrial, electronic and power equipment cooling applications. The flow of air in the channel is induced by the thermal buoyancy force. A low Reynolds number k–ε turbulence model is used in conjunction with heat transfer analysis in the channel. The model predictions are first compared with available experimental data for the purpose of validating the model. Then, the local heat flux and Nusselt number distributions are presented to obtain understanding of the physical phenomena and scaling relations for induced flow rate and average heat transfer coefficient are developed in terms of relevant dimensionless parameters. © 1997 Elsevier Science Ltd.

INTRODUCTION

Vertical two-dimensional channels (slots) formed by parallel plates are frequently encountered configurations in natural convection air cooling of electronic equipment, ranging from transformers to mainframe computers, from transistors to power supplies and cooling of nuclear reactor fuel elements to cooling of containment [1–4]. When two vertical, parallel plates are placed facing each other in an infinite volume of fluid with at least one of them heated, the natural convection flow is induced between the plates due to the buoyancy generated by heating the fluid.

Heat transfer by natural convection from vertical plates with uniform wall temperature or heat flux have received considerable research attention and an extensive discussion is available [5]. Up to date literature citations can be found in more recent publications [6–8]. In summary, the majority of studies have been theoretical for laminar flow. Only a few studies have been reported for turbulent flow. Miyamoto *et al.* [9] studied experimentally turbulent natural convection low and heat transfer in an asymmetrically heated vertical, parallel-plate channel. Local velocity and temperature distributions and heat transfer measurements were reported. Theoretical analysis of turbulent flow and heat transfer in a channel have also been reported [4, 10]. However, no scaling relations for natural convection flow and heat transfer in a vertical, parallel-plate channel have been identified. For the sake of completeness, a few theoretical studies concerned with laminar natural convection transport should be mentioned. Natural convection heat transfer in an asymmetrically heated, vertical, parallel-plate channel, with one wall heated by a uniform flux and the other thermally insulated, has been studied by Miyatake *et al.* [11]. Natural convection flow and heat transfer between vertical plates at unequal temperatures [12], with one plate isothermally heated and the other plate insulated [13], have also been investigated. Reference is made to Ramanathan and Kumar [6] for a more complete list of studies on laminar natural convection between heated vertical plates.

The present theoretical study is concerned with turbulent natural convection in an asymmetrically heated vertical, parallel-plate channel. The aim is to gain improved understanding of turbulent flow and thermal structures and to develop scaling relations for natural convection heat transfer. To this end, the low Reynolds number k–ε turbulence model is used to simulate turbulent flow. Numerical results are reported for dry air as the coolant.

ANALYSIS

Physical model, assumptions and model equations

Consider an asymmetrically heated vertical, parallel-plate channel shown schematically in Fig. 1. The left wall of the channel is heated by imposing a uniform wall temperature or heat flux. The right wall of the channel (slot) is adiabatic. Air enters the channel at temperature T_o. We consider the case where the thermal buoyancy force drives the fluid motion. The transport processes are considered steady and the flow incompressible. Radiation heat transfer is neglected.

† Author to whom correspondence should be addressed.

NOMENCLATURE

C_1, C_2, C_3, C_μ	empirical constants in the k-ε turbulence model
c_p	specific heat
D_h	hydraulic diameter
f_1, f_2, f_μ	functions in the k–ε turbulence model
G	generation term in turbulence equations, equation (7)
Gr	Grashof number, $g\beta\Delta TW^3/\nu^2$
H	height of the parallel-plate channel (see Fig. 1)
h	heat transfer coefficient
k	kinetic energy of turbulence or thermal conductivity
Nu	Nusselt number, equation (15)
Pr	Prandtl number, $\mu c_p/k$ or ν/α
Pr_t	turbulent Prandtl number, $\mu_t c_p/k_t$
q	heat flux, equation (13)
Re	Reynolds number, $\rho_0 v_0 D_h/\mu$
Re_t	turbulent Reynolds number, $k^2/\varepsilon\nu$
T	tempeature
Tu	turbulent intensity
u	horizontal velocity component in the x-direction
v	vertical velocity component in the y-direction
W	channel width (see Fig. 1)
x	coordinate as defined in Fig. 1
y	coordinate as defined in Fig. 1.

Greek symbols

α	thermal diffusivity, $k/\rho c_p$
ε	dissipation rate of turbulent kinetic energy
μ	dynamic viscosity
ν	kinematic viscosity
ρ	density
σ_k, σ_ε	turbulent Prandtl number for k and ε, respectively.

Subscripts

b	refers to bulk gas
c	refers to cold wall
H	refers to height of channel (see Fig. 1)
h	refers to hot wall
k	refers to kinetic energy
s	refers to sensible
t	refers to turbulent quantity
w	refers to heated wall
y	refers to local quantity along y-coordinate
o	refers to inlet of channel.

Superscripts

–	averaged quantity
′	fluctuating quantity.

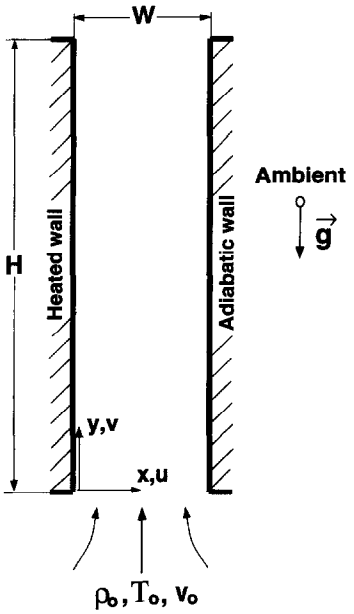

Fig. 1. Schematic diagram and coordinate system for natural convection transport in a vertical, parallel-plate channel.

The time-averaged Navier–Stokes equations of motion for steady, two-dimensional incompressible flow in a vertical channel can be written as:

Conservation of mass (continuity)

$$\frac{\partial(\rho u)}{\partial x}+\frac{\partial(\rho v)}{\partial y}=0. \tag{1}$$

Conservation of x*-momentum*

$$\frac{\partial}{\partial x}(\rho uu)+\frac{\partial}{\partial y}(\rho uv)=-\frac{\partial p}{\partial x}+\frac{\partial}{\partial x}\left[(\mu+\mu_t)\frac{\partial u}{\partial x}\right]+\frac{\partial}{\partial y}\left[(\mu+\mu_t)\frac{\partial u}{\partial y}\right]-\frac{2}{3}\rho\frac{\partial k}{\partial x}. \tag{2}$$

Conservation of y*-momentum*

$$\frac{\partial}{\partial x}(\rho uv)+\frac{\partial}{\partial y}(\rho vv)=-\frac{\partial p}{\partial y}+\frac{\partial}{\partial x}\left[(\mu+\mu_t)\frac{\partial v}{\partial x}\right]+\frac{\partial}{\partial y}\left[(\mu+\mu_t)\frac{\partial v}{\partial y}\right]-\frac{2}{3}\rho\frac{\partial k}{\partial y}+(\rho-\rho_o)g. \tag{3}$$

Conservation of energy equation

$$\frac{\partial}{\partial x}(\rho uT)+\frac{\partial}{\partial y}(\rho vT)=\frac{\partial}{\partial x}\left[\left(\frac{k}{c_p}+\frac{\mu_t}{Pr_t}\right)\frac{\partial T}{\partial x}\right]+\frac{\partial}{\partial y}\left[\left(\frac{k}{c_p}+\frac{\mu_t}{Pr_t}\right)\frac{\partial T}{\partial y}\right]. \quad (4)$$

The superscript bar (¯) usually employed to denote time-averaged dependent variables is neglected for the sake of simplicity in notation. The turbulent dynamic viscosity μ_t is to be predicted from the knowledge of the kinetic energy of turbulence k and turbulent kinetic energy dissipation rate ε. Note that in the above formulation the variation of the thermophysical properties (density, viscosity and thermal conductivity) with temperature has been accounted for using published information [14].

The transport equations for k and ε are formulated using the low Reynolds number k–ε turbulence model. These equations can be derived from the Navier–Stokes equations of motion and are given as [15, 16].

Turbulence kinetic energy (k-*equation*)

$$\frac{\partial}{\partial x}(\rho uk)+\frac{\partial}{\partial y}(\rho vk)=\frac{\partial}{\partial x}\left[\left(\mu+\frac{\mu_t}{\sigma_k}\right)\frac{\partial k}{\partial x}\right]+\frac{\partial}{\partial y}\left[\left(\mu+\frac{\mu_t}{\sigma_k}\right)\frac{\partial k}{\partial y}\right]-\rho\varepsilon+\frac{g}{\rho}\left(\frac{\mu_t}{Pr_t}\right)\frac{\partial \rho}{\partial y}+G. \quad (5)$$

Kinetic energy of turbulence dissipation (ε-*equation*)

$$\frac{\partial}{\partial x}(\rho u\varepsilon)+\frac{\partial}{\partial y}(\rho v\varepsilon)=\frac{\partial}{\partial x}\left[\left(\mu+\frac{\mu_t}{\sigma_\varepsilon}\right)\frac{\partial \varepsilon}{\partial x}\right]+\frac{\partial}{\partial y}\left[\left(\mu+\frac{\mu_t}{\sigma_\varepsilon}\right)\frac{\partial \varepsilon}{\partial y}\right]+C_1 f_1(\varepsilon/k)G-C_2 f_2\rho\varepsilon^2/k+C_3\frac{g}{\rho}\left(\frac{\mu_t\varepsilon}{Pr_t k}\right)\frac{\partial \rho}{\partial y} \quad (6)$$

where

$$G=\mu_t\left(\frac{\partial u_i}{\partial x_j}+\frac{\partial u_j}{\partial x_i}\right)\frac{\partial u_i}{\partial x_j}-\frac{2}{3}k\delta_{ij}\frac{\partial u_i}{\partial x_j}. \quad (7)$$

In the conservation equations and the k–ε turbulence model equations, the turbulent dynamic (eddy) viscosity for momentum, μ_t, is related to k and ε by

$$\mu_t=C_\mu\rho f_\mu(k^2/\varepsilon). \quad (8)$$

The appropriate constants, factors, turbulent Prandtl and Schmidt numbers, as well as the low Reynolds number wall damping functions, f_μ, f_1 and f_2 are not well-known for turbulent, buoyancy-driven convective flows, although they have been generated and optimized for forced convection boundary layer flows [17–19]. A recent discussion of low Reynolds number k–ε turbulence models for forced flows in pipes is available [20]. Reference is made to Perez-Segarra *et al.* [21] for a comprehensive citation of studies which have employed the low Reynolds number k–ε turbulence model to simulate transport under natural convection conditions. For lack of a better choice, these results for forced convection flows are retained in the present analysis for natural convection. The values of constants and functions are listed in Table 1.

Table 1. The constants and functions for the low Reynolds number k–ε turbulence model

C_1	C_2	C_3	C_μ	Pr_t	σ_k	σ_ε
1.44	1.8	1.5	0.09	0.9	1.0	1.3
f_1	1.0					
f_2	$1.0-0.3\exp(-Re_t^2)$					
f_μ	$\exp[-3.4/(1-Re_t/50)^2]$					

As the flow involves combined heat and mass transfer, the turbulent Prandtl number must be specified. Calculations with a constant value of $Pr_t = 0.9$ across the boundary layer show no pronounced effect on the heat transfer coefficient (i.e. Stanton number) and temperature distributions [18]. Therefore, a value of $Pr_t = 0.9$ is used in the calculations.

Boundary conditions

A no-slip boundary condition is imposed on the velocity components at the walls. The velocity at the inlet is computed from a mass balance and the velocity gradient is set to zero at the outlet. Either a uniform heat flux or a uniform temperature boundary condition is imposed at the heated, left wall of the channel. The boundary conditions for k and ε at the wall, consistent with the equations for the low Reynolds number k–ε turbulence model, are [15]

$$k=0 \quad \text{at walls} \quad (9)$$

$$\varepsilon=2(\mu/\rho)\left(\frac{\partial k^{1/2}}{\partial x}\right)^2 \quad \text{at walls.} \quad (10)$$

The kinetic energy of turbulence at the inlet ($y = 0$) is expressed as

$$k=k_o=\frac{3}{2}Tu_o v_o^2 \quad (11)$$

where Tu_o is the turbulence intensity at the channel inlet. The turbulent kinetic energy dissipation rate, ε, at the inlet is given by

$$\varepsilon_o=(\mu/\rho)\left(\frac{C_\mu}{\kappa}\right)\left(\frac{\rho k_o^{3/2}}{\mu x_w}\right) \quad (12)$$

where x_w is the distance measured from the wall. The air temperature at the inlet to the channel is specified to be the ambient temperature and the temperature gradient is assumed to vanish at the exit of the channel.

Heat transfer parameters

The local heat exchange from the heated wall to the air stream depends on the temperature gradient on

the air side. The convective heat transfer flux from the heated wall to the dry air stream can be expressed in terms of the local heat transfer coefficient (h_y) as

$$q_w(y) = -k\frac{\partial T}{\partial x} = h_y[T_w(y) - T_b(y)] \quad \text{at} \quad x = 0 \tag{13}$$

where the subscript 'w' denotes the quantities at the hot wall and the local bulk temperature T_b in the channel is defined as

$$T_b(y) = \int_0^W \rho c_p v T \, dx \int_0^W \rho c_p v \, dx. \tag{14}$$

For the purpose of generalizing the heat transfer results, the local Nusselt number along the hot wall is defined as

$$Nu_y = \frac{h_y D_h}{k} = \frac{2Wq_w}{k[T_w(y) - T_b(y)]} = -\frac{2W(\partial T/\partial x)_w}{[T_w(y) - T_b(y)]}. \tag{15}$$

Method of solution

A finite-difference numerical solution technique based on integration over the control volume is used to solve the model equations with appropriate boundary conditions. The SIMPLER algorithm is employed to solve the model equations in primitive variables and this is discussed in detail by Patankar [22]. The application of the method to the solution of the transport equations under the natural convection conditions is detailed elsewhere [23] and does not need to be repeated here. Suffice to mention that final converged steady-state solutions were obtained by solving iteratively the unsteady transport equations with very large pseudo-time steps. The fully implicit Euler method was used to march the solution in pseudo-time. The thermophysical properties (density, viscosity and thermal conductivity) were evaluated explicitly, based on the temperature from the previous iteration (pseudo-time step). In order to improve the resolution of dependent variables in the turbulent boundary layers a non-uniform grid has been employed [23]. Grid independence of the results was established by employing different size meshes, ranging in size from 51×101 to 101×401.

The turbulent k- and ε- equations are homogeneous. Therefore, the initial values for turbulent kinetic energy k and its dissipation rate, ε, must be specified in order to start the iterative calculations. In all results presented the initial distributions for k and ε were assumed to be uniform and equal to 10^{-3} and 10^{-5}, respectively. No special models have been utilized to trigger transition to turbulence at some specific location in the flow field. In the results presented the transition from the laminar to the turbulent regime occurs naturally as the solution of the governing transport equations.

It is necessary to mention that the SIMPLER method adopted for the numerical solution of the transport equations is not extremely robust for low Reynolds number of mixed convection flows and the intimate coupling of model equations cause additional difficulties. In addition, the k–ε turbulence model equations are highly nonlinear and must be solved simultaneously with the transport equations. This required a large number of iterations (pseudo-time steps) to obtain converged solutions.

RESULTS AND DISCUSSION

Comparison of model predictions with experimental data

Experimental data have been reported by Miyamoto *et al.* [9] on turbulent natural convection flow and heat transfer in an asymmetrically heated vertical channel. The channel was formed by two vertical parallel plates. One plate was heated by imposing a uniform heat flux along the plate and the opposite plate was adiabatic. The channel under investigation was 4980 mm high and spanned 950 mm. The channel was open at the bottom and top and was installed in a laboratory room which was 6107 mm high. Experiments were performed with channel widths of 50, 100 and 200 mm, and local heat transfer coefficients were determined at the heated wall. The experimental data reported can be used to check the validity and appropriateness of the turbulent, two-dimensional flow and heat transfer model developed.

The theoretically predicted kinetic energy of turbulence $k[=(u'^2+v'^2+w'^2)/2]$ per unit mass and the experimentally measured component distributions are illustrated in Fig. 2. The w'^2 was not reported by Miyamoto *et al.* [9], but it is believed to be much smaller than v'^2. Since the u'^2 and v'^2 were not measured at the same spatial locations across the channel, no attempt is made to add the two components. However, experimental data clearly show that the longitudinal pulsation component (v'^2) prevails over the cross-stream one (u'^2). The turbulence intensity and instantaneous (fluctuating) air temperature upstream of the channel inlet were not measured and reported by Miyamoto *et al.* [9], therefore, the calculations were performed and are presented in Fig. 2 for four different turbulence intensities upstream of the channel inlet (i.e. $Tu_o = 0$, 10, 15 and 20%). Comparison of predictions with the data shows that the agreement between them is best when the turbulence intensity at the inlet to the channel Tu_o is 15%. The low Reynolds number k–ε turbulence model adopted appears to be capable of simulating the turbulence characteristics in an asymmetrically heated vertical, parallel-plate channel under buoyancy driven flow conditions.

Figure 3 shows a comparison between the measured and theoretically predicted wall temperatures along the heated wall of the channel. The results show that for $Tu = 0\%$ the wall temperature is overpredicted for $0.4 < y < 4$ m compared to the measured data

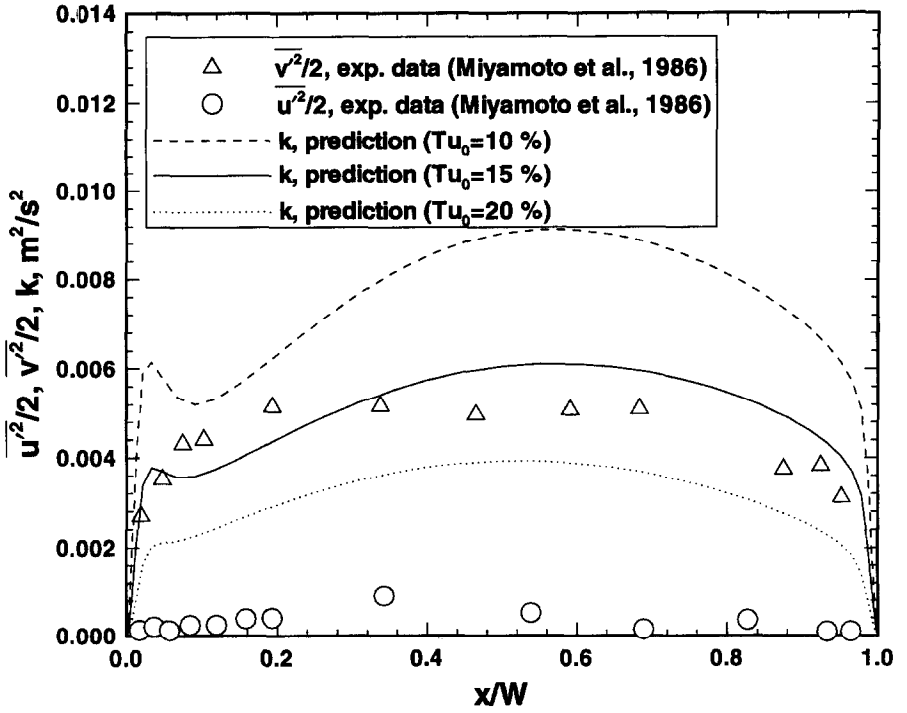

Fig. 2. Effect of turbulence intensity at inlet to a channel on kinetic energy of turbulence for $q_w = 104$ Wm^{-2} and $W = 0.1$ m.

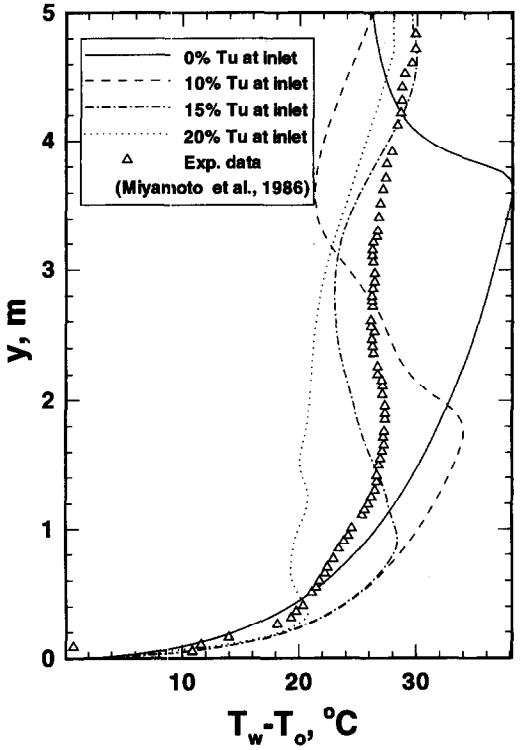

Fig. 3. Comparison of predicted and measured wall temperature variations along a heated vertical wall for $q_w = 104$ Wm^{-2} and $W = 0.1$ m.

and the transition from laminar to turbulent flow is predicted too late ($y > 3.6$ m) up along the channel wall. The wall temperature is overpredicted by about a maximum of 36% at $y = 3.7$ m. Of the three remaining cases (i.e. $Tu_o = 10$, 15 and 20%), the agreement between the calculated and measured wall temperatures appears to be the best for $Tu_o = 15\%$. This finding supports the conclusion reached when discussing the calculations of the kinetic energy of turbulence k in the preceding paragraph and further refinement of Tu_o values at inlet is not warranted. The comparison shown in the figure is quite critical and the reasonably good agreement of data with predictions provides some additional confidence in the model capabilities.

A comparison between the predicted and measured mean (i.e. time-averaged) vertical velocity distributions at two different heights along the channel is given in Fig. 4 and it is made for one of three experiments for which the velocity data were reported by Miyamoto *et al.* [9]. The calculations were performed by assuming that the turbulence intensity upstream of the channel inlet was 15%. During the course of the numerical iterations, the flow rates indicated a low frequency 'oscillations' in the overall mass balance for the channel. The velocities reported in the figure are the results at the iteration number 1000. Close to the exit of the channel, at $y = 3.865$ m, the flow is nearly developed and the vertical velocity profile predicted is very smooth (see Fig. 4(b)). Also, the predictions are in surprisingly good agreement with the measured data for both locations. In the vicinity of the heated left wall the vertical velocity is somewhat overpredicted, but in the vicinity of the adiabatic right wall the velocity is underpredicted; however, in general, the measured and calculated average vel-

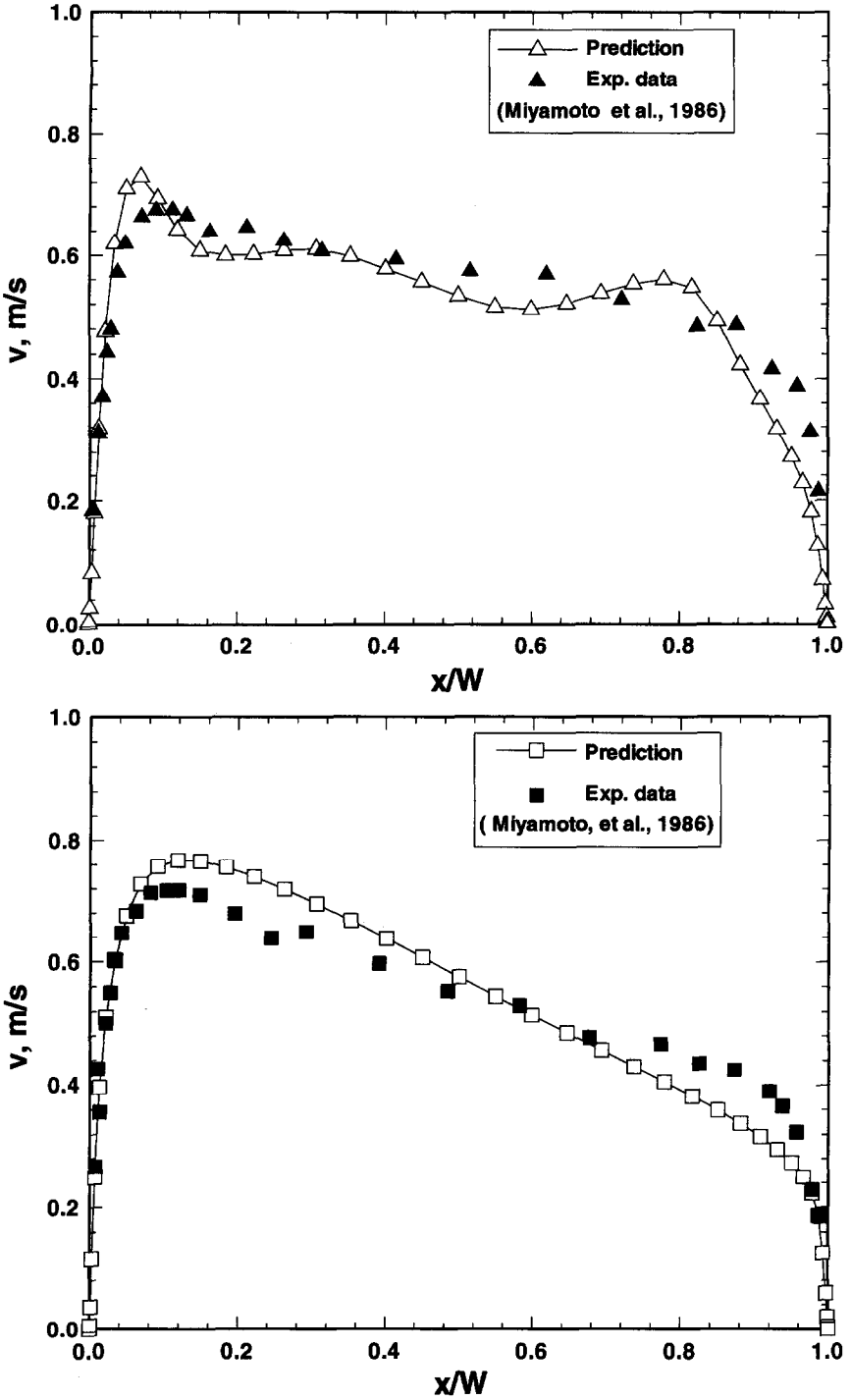

Fig. 4. (a) Comparison of predicted and measured vertical velocity component distributions in an asymmetrically heated, vertical parallel-plate channel for $q_w = 208$ Wm^{-2}, $W = 0.1$ m, $y = 0.820$ m and $Tu_o = 15\%$. (b) Comparison of predicted and measured vertical velocity component distributions in an asymmetrically heated, vertical parallel-plate channel for $q_w = 208$ Wm^{-2}, $W = 0.1$ m, $y = 3.865$ m and $Tu_o = 15\%$.

ocities are in good agreement with each other. Note also that the velocity profile calculated is not symmetric about the central plane of the channel (i.e. is considerably) owing to asymmetric heating.

The bulk streamwise velocity ($v_b = \int_0^W \rho v \, dx / \int_0^W \rho \, dx$) at the location $y = 3.865$ m [$v_o(y = 3.865$ m$) = 0.583$ ms^{-1}] is larger than that at $y = 0.820$ m [$v_b(y = 0.820$ m$) = 0.571$ ms^{-1}] owing to an increase in the average fluid temperature in the downstream direction. The difference is relatively small because

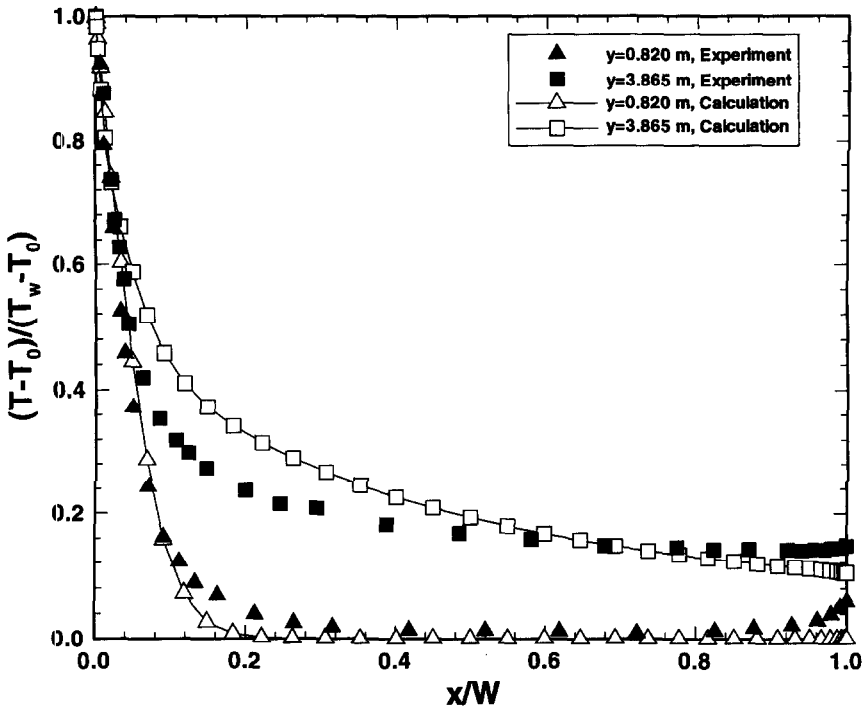

Fig. 5. Comparison of predicted and measured temperature distributions in an asymmetrically heated, vertical parallel-plate channel for $q_w = 208$ Wm^{-2}, W = 0.1 m, and $Tu_o = 15\%$.

the bulk temperature increases only modestly [from $T_b(y = 0.820$ m) = 14.59°C to $T_b(y = 3.865$ m) = 21.82°C]. However, Fig. 4 reveals that the velocity distribution at $y = 0.820$ m is 'wrinkling' and there is a region in the vicinity of the adiabatic (cold) wall ($0.6 < x/W < 0.85$) where the local velocity at $y = 0.820$ m is larger than the local velocity at $y = 3.856$ m. This behavior is attributed to the fact that the flow transitions from laminar to turbulent at $0.8 \lesssim y \lesssim 0.9$ m. The heat and momentum transport mechanisms in this region are very complex and cannot be readily explained through the basic concepts of thermal buoyancy induced flow.

A comparison of the measured and predicted temperature distributions in the air at two vertical locations along the channel is shown in Fig. 5. The results are for the same experiment for which the vertical velocity component profiles were discussed in the preceding paragraph. The experimental data reveal greater turbulent mixing than predicted by the model calculations. The numerical results are based on the assumption of an adiabatic right ($x/W = 1.0$) wall, but radiation from the hotter left wall ($x/W = 0$) apparently heated the right wall and made it non-adiabatic. This is clearly indicated by a small rise in the experimental air temperature data in the vicinity of the right wall. However, despite these differences the measured and predicted temperature gradients in air at the hot wall are in very good agreement with each other. This finding is encouraging and suggests that the low Reynolds number k–ε turbulence model has capability to predict local convective heat flux in an asymmetrically heated vertical channel under natural circulation conditions.

Velocity, temperature and local Nusselt number distributions. Figures 6 and 7 illustrate some typical results for the vertical velocity component and temperature distribution along an asymmetrically heated vertical channel, respectively. The results are for a uniform wall temperature boundary condition and $Tu_o = 0\%$. Even for a very large aspect ratio ($H/W = 80$) channel, the velocity profile is not fully developed. The velocity profile still changes from $y/H \approx 71$ to $y/H = 80$ (Fig. 6). The results also show that the velocity profile is not symmetrical about the midplane $x/W = 0.5$ of the channel. This is due to the fact that the local buoyancy force is larger near the hot (left) wall than near the adiabatic (right) wall. As is evident from the temperature profiles shown in Fig. 7, the local buoyancy force continues to change even near the top of the channel ($70 < y/H < 80$) as the bulk temperature increases with the distance from the inlet of the duct. The temperature profiles near the hot wall reveal that there is a transition from laminar to turbulent flow at $y/H \simeq 50$. At this location the temperature gradient increases rather abruptly confirming the transition; unfortunately, because of the density of the curves in the immediate vicinity of the hot wall these changes in the thermal structure cannot be clearly revealed.

The local Nusselt number distributions along the heated wall of the channel are illustrated in Fig. 8. The results show that for $Gr = 2 \times 10^5$ and $Tu_o = 0\%$ the flow is still laminar even at the top of the channel,

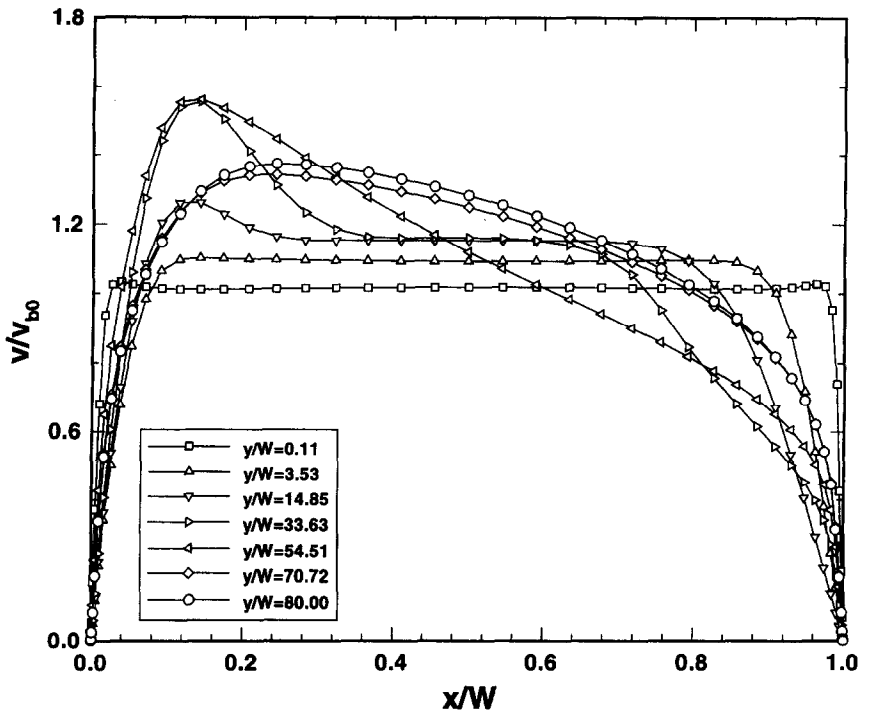

Fig. 6. Predicted distributions of the vertical velocity component in an asymmetrically heated, vertical parallel-plate channel for $Gr = 6 \times 10^5$, $Pr = 0.707$, $H/W = 80$, $T_w = 80°C$, $Tu_o = 0$, and $v_{bo} = 1.173\ ms^{-1}$.

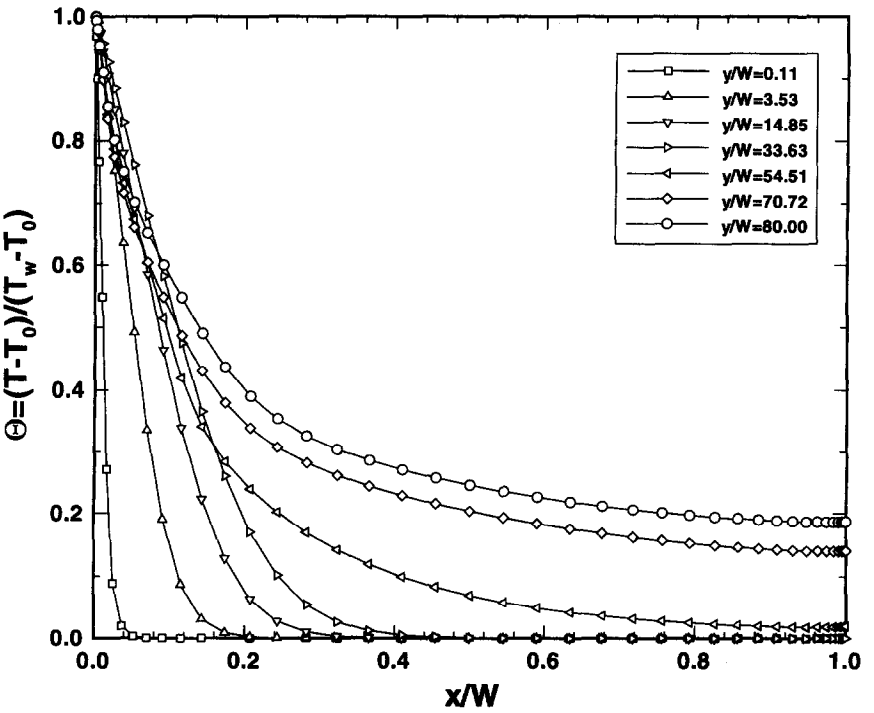

Fig. 7. Predicted temperature distributions in an asymmetrically heated, vertical parallel plate channel for conditions of Fig. 6.

but for $Gr = 4 \times 10^5$ the flow transitions from laminar to turbulent at $y/H = 0.84$, and this is clearly revealed by the sudden increase in the local Nusselt number. As the Grashof number is increased further, the point of transition moves closer to the inlet of the channel. For $Gr = 1 \times 10^6$ the transition will take place at $y/H = 0.64$. An increase in the intensity of turbulence at the inlet to the channel (Tu_o) moves the transition

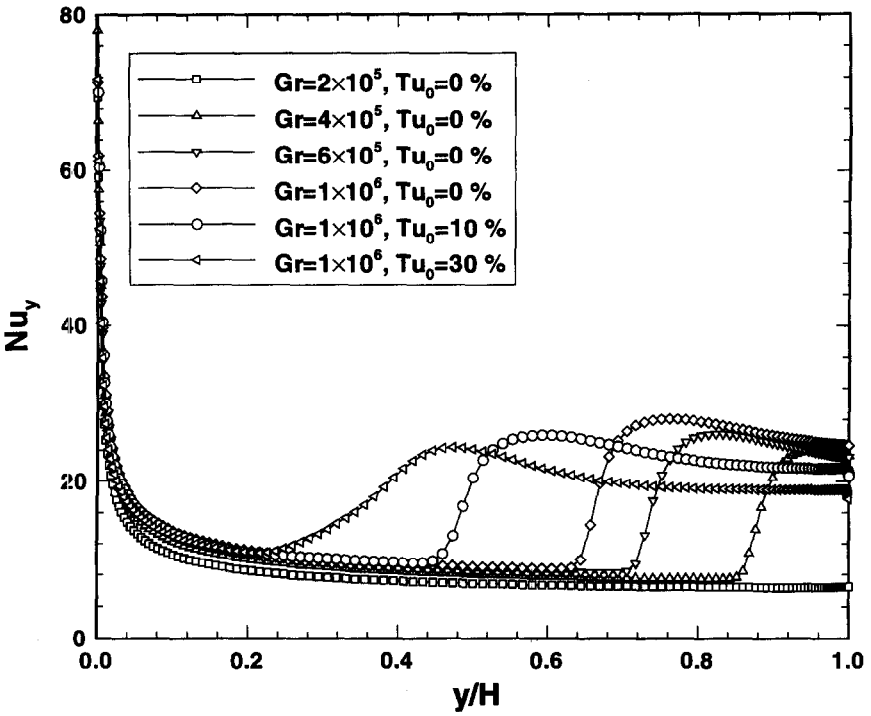

Fig. 8. Effect of the Grashof number and the turbulence intensity at the inlet to the channel on the local Nusselt number distributions along a heated wall for a channel having an aspect ratio $H/W = 80$.

point even further upstream. It is expected that for very high Grashof numbers the flow would be turbulent at or near the inlet to the channel.

Scaling relations. In order to develop some more general understanding of the flow and heat transfer in an asymmetrically heated, vertical parallel-plate channel under natural circulation conditions, extensive parametric calculations were performed. The laminar, transition and eventually fully turbulent flow regimes were present in the channel under the physical conditions analyzed. The averaged results were plotted to obtain some relevant scaling relations. Figure 9 shows the dependence of induced mass flow rate (proportional to the Reynold number Re) vs the Grashof number ($Gr = g\beta\Delta TW^3/\nu^2$), which is related to the buoyancy driving force. In this plot the data could not be represented as a function of the scaling parameter $Gr(W/H)$ alone. The data cannot collapse onto a single line, as the aspect ratio of the channel H/W appears to be an additional correlating parameter. However, there is an asymptotic limit depicted by the continuous straight line which is defined by the results for higher Grashof numbers within each set of aspect ratios H/W.

A somewhat different representation of the induced flow rate (i.e. also induced mean vertical velocity in the channel) is given in Fig. 10. A much better correlation of the results is obtained and numerical data for different aspect ratios collapse onto a single line. In this dimensionless form, the induced air flow rate in the channel can be correlated by the empirical equation

$$Re/(2Gr) = 1.95[GrPr(W/H)]^{-4/5}$$

$$\text{or} \quad Re/Gr = 3.9[GrPr(W/H)]^{-4/5}. \quad (16)$$

The above equation is identical to the one proposed by Miyamoto *et al.* [9] for flow induced along a vertical channel with one wall heated uniformly by imposing a constant heat flux boundary condition. The equation also agrees well with experimental data of Miyatake *et al.* [9], available numerical results for small $GrPr(W/H)(< 1 \times 10^4)$ and numerical predictions for laminar free convection from a single vertical plate with an imposed uniform heat flux [24]. Equation (16) reveals that the induced mass flow rate in the channel ($\rho_o v_o$) depends on temperature difference ΔT and geometrical parameters as follows:

$$\rho_o v_o \sim (\Delta T/WH)^{1/5}(H/W). \quad (17)$$

The dependence of the average Nusselt number ($Nu = \int_0^H Nu_y \, dy/H$) on the buoyancy force parameter $[GrPr(W/H)]$ is illustrated in Fig. 11. All of the data for different aspect ratio channels are correlated by an empirical equation

$$Nu = 2.10[GrPr(W/H)]^{1/5}. \quad (18)$$

The above equation is a least-squares fit of the data for the range of parameters investigated. Note that Tu_o was set to be equal 0%.

For an identical physical situation, but for laminar flow, Miyatake and Fujii [13] obtained the following empirical correlation for the average Nusselt number

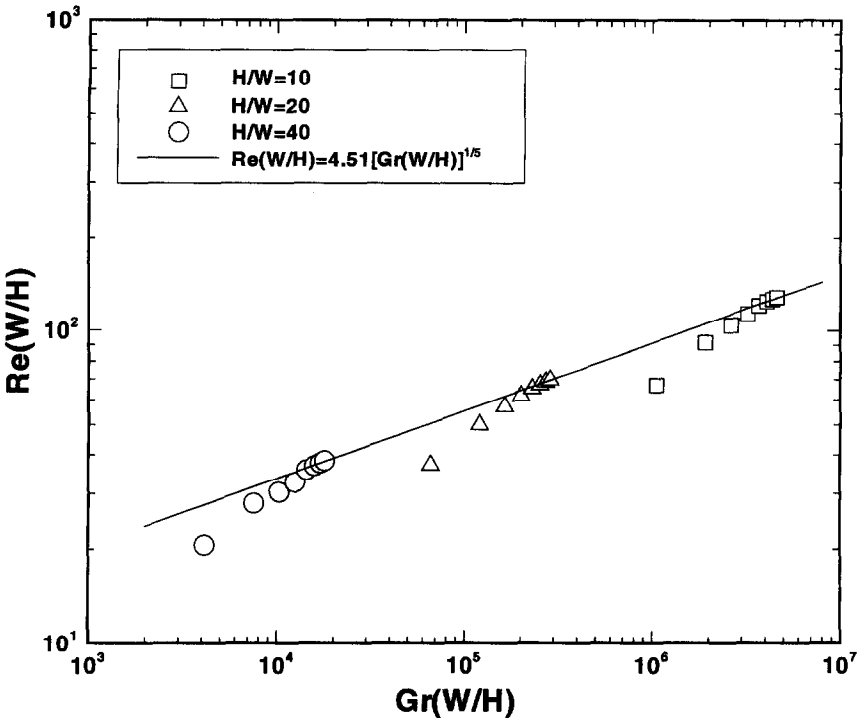

Fig. 9. Dependence of dimensionless induced flow rate (mean velocity) on the buoyancy driving force (Gr) for $Tu_o = 0$.

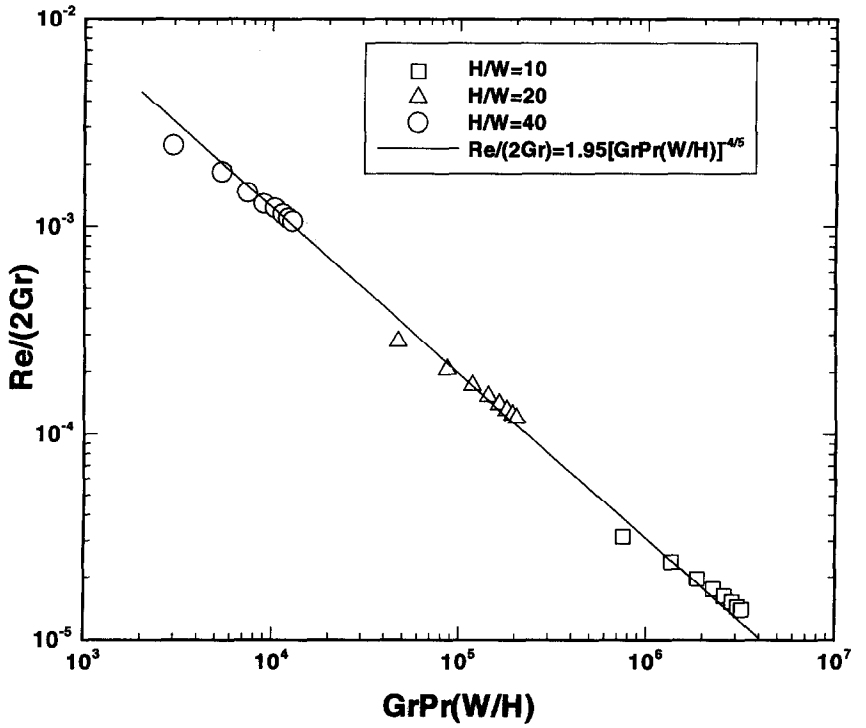

Fig. 10. Effect of the dimensionless induced flow rate on the dimensionless buoyancy force for $Tu_o = 0$.

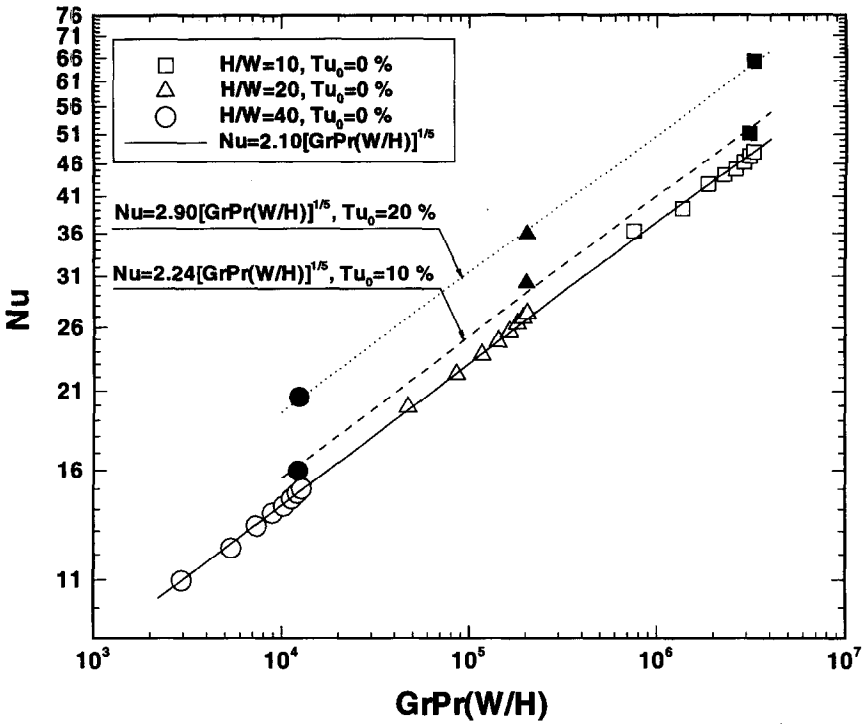

Fig. 11. Variation of the dimensionless average heat transfer coefficient (Nu) along the heated vertical wall with the dimensionless buoyancy force (Gr) for different inlet turbulence intensities (Tu_0).

$$Nu = 0.613[GrPr(W/H)]^{1/4}. \quad (19)$$

This expression is valid for $Pr = 0.7$. For small $GrPr(W/H) < 1$, the average Nusselt number is given by

$$Nu = \frac{1}{12} GrPr(W/H). \quad (20)$$

As $GrPr(W/H)$ increases the slope decreases from unity as given by the above equation to 1/4 as indicated by equation (19) at $GrPr(W/H) = 300$. Miyatake and Fujii [13] have shown that there is very little effect of the inlet velocity profile on the average Nusselt number for $Pr = 0.7$.

Equation (18) shows that the average heat transfer coefficient along the heated wall of the channel for the turbulent natural convection is given by the following dependence

$$\bar{h} \propto (\Delta T/WH)^{1/5}. \quad (21)$$

Note that the induced mass flow rate and the average convective coefficient increases with the temperature difference between the hot wall and the ambient air temperature, but this dependence is rather weak (i.e. $\sim \Delta T^{1/5}$). It should also be emphasized that the correlating equation was derived by neglecting radiation heat exchange between the heated and the adiabatic walls. At large ΔTs radiation heat exchange between the two walls will become significant. The right ('adiabatic') wall will be heated and the assumption that it is insulated will no longer be appropriate. This is evident from the experimental data shown in Fig. 5 and was discussed in detail in the respective subsection.

Another interesting scaling relationship can be obtained by combining equations (17) and (21), i.e.

$$\bar{h} \sim \rho_o v_o (H/W)^{-1}. \quad (22)$$

It means that the average heat transfer coefficient for the buoyancy driven flow in the vertical parallel-plate channel is proportional to the induced mass flow rate and inversely proportional to the channel aspect ratio.

The effect of the turbulence intensity at inlet to the channel Tu_o has also been investigated and the results are summarized in Fig. 11. As expected, inlet turbulence increases Nusselt numbers and the increase in nonlinear. The results show that the functional dependence of Nu vs $GrPr(W/H)$ is not affected by Tu_o as the slope of the straight lines remains the same and only the coefficient is increased by increasing Tu_o.

CONCLUSIONS

Turbulent buoyancy-driven flow and heat transfer characteristics in an asymmetrically heated, vertical parallel-plate channel force have been studied. Based on the numerical results obtained the following conclusions can be drawn:

(1) Comparison of the available experimental data and model prediction suggests that the low Reynolds number k–ε turbulence model is capable

of predicting heat transfer in thermal buoyancy-driven flows.

(2) The turbulence intensity at the inlet to the channel affects the location of transition from laminar to turbulent flow as well as the average heat transfer coefficient.

(3) Scaling relations for the Reynolds and average Nusselt numbers have been developed in terms of relevant dimensionless parameters.

(4) Detailed experimental flow, heat and mass transfer data are needed to further validate the two-dimensional transport analysis and the appropriateness of the low Reynolds number k–ε turbulence model. The greatest computational uncertainty is in the prediction of the correct location for transition from laminar to turbulent flow.

Acknowledgements—This work was supported in part by the U.S. Nuclear Regulatory Commission through a contract to Energy Research, Inc. The authors wish to acknowledge the assistance of Professor A. A. Mohamad concerning the model and computer program development and the helpful discussions with Dr M. Khatib-Rahbar, Mr A. Notafrancesco and Dr J. Tills.

REFERENCES

1. Wirtz, R. A. and Stutzman, R. J., Experiments on free convection between vertical plates with symmetric heating. *Journal of Heat Transfer*, 1982, **104**, 501–507.
2. Bar-Cohen, A. and Rohsenow, W. M., Thermally optimum spacing of vertical, natural convection cooled, parallel plates. *Journal of Heat Transfer*, 1984, **106**, 116–123.
3. Betts, P. L. and Dafa'nela, A. A., Turbulent buoyant air flow in a tall rectangular cavity. *ASME*, HTD-Vol. 60, ASME, New York, 1986, p. 83.
4. Cheung, F. B. and Sohn, D. Y., Numerical study of turbulent natural convection in an innovative air cooling system. *Numerical Heat Transfer, Part A*, 1989, **16**, 467–487.
5. Gebhart, B., Jaluria, Y., Mahajan, R. L. and Summakia, B., *Buoyancy-Induced Flows and Transport*. Hemisphere, Washington, DC, 1987.
6. Ramanathan, S. and Kumar, R., Correlations for natural convection between heated vertical plates. *Journal of Heat Transfer*, 1991, **113**, 97–107.
7. Fujii, M., Tomimura, T., Zhang, X. and Gima, S., Numerical convection from an array of vertical parallel plates. In *Heat Transfer*, eds G. F. Hewitt *et al.*, Vol. 7. Institute of Chemical Engineers, Rugby, U.K., 1994, pp. 49–54.
8. Hanjalić, K., Achievements and limitations in modelling and computation of buoyant turbulent flows and heat transfer. In *Heat Transfer*, G. F. Hewitt *et al.*, Vol. 1. Institution of Chemical Engineers, Rugby, U.K., 1994, pp. 1–18.
9. Miyamoto, M., Katoh, Y., Kurima, J. and Saki, H., Turbulent free convection heat transfer from vertical parallel plates. In *Heat Transfer*, eds C. L. Tien, V. P. Carey and J. K. Ferrell, Vol. 4. Hemisphere, Washington, DC, 1986, pp. 1593–1598.
10. Korbut, V. P. and Paladenko, Yu. V., Turbulent natural-convection flow and heat transfer in a flat vertical slot with asymmetrically heated walls. *Heat Transfer Research*, 1993, **25**, 313–320.
11. Miyatake, O., Fujii, T., Fujii, M. and Tanaka, H., Natural convection heat transfer between vertical parallel plates—one plate with a uniform heat flux and the other thermally insulated. *Heat Transfer—Japanese Research*, 1973, **2**(1), 25–33.
12. Miyatake, O. and Fujii, T., Natural convection heat transfer between vertical parallel plates at unequal uniform temperature. *Heat Transfer—Japanese Research*, 1973, **2**(4), 79–88.
13. Miyatake, O. and Fujii, T., Free convection heat transfer between vertical parallel plates—one plate isothermally heated and the other plate insulated. *Heat Transfer—Japanese Research*, 1973, **2**(4), 30–38.
14. Tsay, Y. L. and Lin, T. F., Combined heat and mass transfer in laminar gas stream flowing over an evaporating liquid film. *Wärme-und Stoffübertragung*, 1990, **25**, 221–231.
15. To, W. M. and Humphrey, J. A. C., Numerical simulation of buoyant, turbulent flow—I. Free convection along a heated vertical plate. *International Journal of Heat and Mass Transfer*, 1987, **25**, 221–231.
16. Yan, W.-M., Mixed convection heat and mass transfer in a wetted channel. *Canadian Journal of Chemical Engineering*, 1991, **69**, 1277–1282.
17. Jones, W. P. and Launder, B. E., The calculation of low Reynolds number phenomena with a two-equation model of turbulence. *International Journal of Heat and Mass Transfer*, 1973, **16**, 1119–1130.
18. Patel, V. C., Rodi, W. and Schenerer, G., Turbulence models for near-wall and low Reynolds number flow: a review. *AIAA Journal*, 1985, **23**, 1308–1319.
19. Launder, B. E., On the computation of convective heat transfer in complex turbulent flows. *Journal of Heat Transfer*, 1988, **110**, 1112–1128.
20. Hsieh, W. D. and Chang, K. C., Calculation of wall heat transfer in pipe-expansion turbulent flows. *International Journal of Heat and Mass Transfer*, 1996, **39**, 3813–3822.
21. Perez-Sagarra, C. D., Oliva, A., Costa, M. and Escanes, F., Numerical experiments in turbulent natural and mixed convection in internal flows. *International Journal of Numerical Methods of Heat and Fluid Flow*, 1995, **5**, 13–33.
22. Patankar, S. V., *Numerical Heat Transfer and Fluid Flow*. Hemisphere, Washington, DC. 1980.
23. Mohamad, A. A. and Viskanta, R., Application of low Reynolds number k–ε turbulence model to buoyant and mixed flows in a shallow cavity. In *Fundamentals of Mixed Convection*, eds. T. S. Chen and T. Y. Chen, Vol. HTD-213. ASME, New York, 1992, pp. 43–54.
24. Miyamoto, M., Kajino, H., Kurima, J. and Tanakami, I., Development of turbulence characteristics in a vertical free convection boundary layer. In *Heat Transfer*, eds U. Grigull *et al.*, Vol. 2. Hemisphere, Washington, DC 1982, pp. 323–328.